Acta Crystallographica Section D
Biological Crystallography
ISSN 0907-4449

Cross-linking of protein crystals as an aid in the generation of binary protein–ligand crystal complexes, exemplified by the human PDE10a–papaverine structure

Ole Andreas Andersen,[a] Dorian Leo Schönfeld,[a] Ian Toogood-Johnson,[a] Brunella Felicetti,[a] Claudia Albrecht,[b] Tara Fryatt,[a] Mark Whittaker,[a] David Hallett[a] and John Barker[a]*

[a]Evotec (UK) Ltd, 114 Milton Park, Abingdon, Oxfordshire OX14 4SA, England, and [b]Evotec AG, Schnackenburgallee 114, 22525 Hamburg, Germany

Correspondence e-mail: john.barker@evotec.com

Received 7 April 2009
Accepted 12 May 2009

PDB Reference: PDE10a–papaverine complex, 2wey, r2weysf.

Protein crystallography has proven to be an effective method of obtaining high-resolution structures of protein–ligand complexes. However, in certain cases only apoprotein structures are readily available and the generation of crystal complexes is more problematic. Some crystallographic systems are not amenable to soaking of ligands owing to crystal-packing effects and many protein–ligand complexes do not crystallize under the same conditions as used for the apoprotein. Using crystals of human phosphodiesterase 10a (hPDE10a) as an example of such a challenging crystallographic system, the structure of the complex with papaverine was obtained to 2.8 Å resolution using protein crystals cross-linked by glutaraldehyde prior to soaking of the ligand. Inspection of the electron-density maps suggested that the correct mode of binding was obtained in one of the two monomers in the asymmetric unit and inspection of crystal-packing contacts explained why cocrystallization experiments and soaking of crystals that were not cross-linked were unsuccessful.

1. Introduction

Determination of the detailed mode of ligand binding to a protein by X-ray crystallography requires a protein–ligand crystal complex, which is usually formed by soaking of the ligand into apoprotein crystals or cocrystallization of the complex. Frequently, generation of crystallographic complexes are problematic, while the protein readily crystallizes in its apo form. For example, soaking experiments are often unsuccessful because crystallographic neighbour molecules restrict access to the ligand-binding site. The most common approaches to this problem are to screen for new crystallization conditions in order to acquire a different crystal form of the apoprotein or to acquire conditions for cocrystallization of the binary complex. Here, we present an alternative approach to resolve the complication described above, exemplified by the crystal structure of human phosphodiesterase 10a (hPDE10a) complexed with papaverine. Phosphodiesterases hydrolyse the second messengers cyclic AMP and cyclic GMP which are ubiquitous in mammalian tissues and thus regulate various cellular functions (reviewed in Lugnier, 2006). Most inhibitors that are selective for other phosphodiesterase families are poor inhibitors of phosphodiesterase 10a (PDE10a); however, the specific and potent PDE10a inhibitor papaverine has been extensively used as a pharmacological tool to investigate the effects of PDE10a inhibition *in vitro* and *in vivo*. For example, papaverine is effective in animal models predictive of antipsychotic activity, suggesting that inhibition of the enzyme may represent a novel approach to the treatment of psychosis (Siuciak *et al.*, 2006). Crystal structures of human (Wang *et al.*, 2007) and rat PDE10a have recently been published (Chappie *et al.*, 2007); however, no structure of any phosphodiesterase in complex with papaverine has been reported to date. Extensive soaking and cocrystallization experiments to obtain a complex of hPDE10a with papaverine were unsuccessful. Consequently, hPDE10a crystals were cross-linked using glutaraldehyde (for glutaraldehyde reaction mechanisms, see Wine *et al.*, 2007) to prevent crystal cracking upon soaking with papaverine and the structure of the complex was subsequently solved to 2.8 Å resolution.

2. Materials and methods

2.1. Cloning, expression and purification of hPDE10a and generation of cross-linked hPDE10a crystals complexed with papaverine

The gene coding for the C-terminal catalytic domain of hPDE10a (residues Ser449–Asp789) was amplified by PCR and cloned into the pET15b vector for expression in *Escherichia coli*. The protocols for expression, purification and biochemical assays will be reported elsewhere. The applied procedure generated a catalytically active and monodisperse sample which subsequently proved to be suitable for crystallographic studies.

hPDE10a was crystallized in 14–19% PEG 3350, 200 m*M* $MgCl_2$, 60 m*M* 2-mercaptoethanol and 100 m*M* HEPES pH 7.25 at 278 K (Wang *et al.*, 2007). 2 µl 25% glutaraldehyde at pH 3 was added to a sitting-drop plateau in a well containing the reservoir solution and the well was subsequently sealed with a cover slip holding a crystallization drop with hPDE10a crystals (Lusty, 1999). Crystals were tested at different time intervals of cross-linking to find the minimum time needed to generate crystals able to withstand papaverine soaking and thus minimizing the extent of nonspecific cross-linking. The reaction was allowed to proceed for 15 min. Shorter reaction times did not improve the diffraction quality of the crystals. Cross-linked crystals were subsequently soaked with 16% PEG 8000, 100 m*M* $MgCl_2$, 60 m*M* 2-mercaptoethanol, 100 m*M* HEPES pH 7.25, 4 m*M* papaverine and 4% DMSO for 6 h. Crystals were flash-frozen in 16% PEG 3350, 200 m*M* $MgCl_2$, 60 m*M* 2-mercaptoethanol, 100 m*M* HEPES pH 7.25 and 25%(*v*/*v*) ethylene glycol.

2.2. Structure determination and refinement

Data for the hPDE10a–papaverine structure were collected using a rotating-anode generator with a wavelength of 1.5418 Å. A total of 360 successive images of 0.5° rotation were collected at cryogenic temperature using a single crystal of approximate dimensions 200 × 50 × 50 µm. Processing and scaling of the data were performed using *MOSFLM* (Leslie, 2006) and *SCALA* (Evans, 2006) and the structure was solved by molecular replacement using *MOLREP* (Vagin & Teplyakov, 1997) with PDB entry 2oup (Wang *et al.*, 2007) as a search model. Refinement and model building were completed using *REFMAC*5 (Murshudov *et al.*, 1997) and *Coot* (Emsley & Cowtan, 2004), respectively. Table 1 shows the data-collection and refinement statistics.

Table 1
Summary of data-collection and refinement statistics.

Values in parentheses are for the last resolution shell.

Space group	$P2_12_12_1$
Unit-cell parameters (Å)	a = 50.840, b = 81.570, c = 157.550
Resolution range (Å)	57–2.80 (2.95–2.80)
No. of unique reflections	16777 (2349)
Multiplicity	6.5 (5.9)
Completeness (%)	100.0 (100.0)
R_{merge}† (%)	13.6 (69.4)
Mean $I/\sigma(I)$	13.3 (2.2)
R_{work}‡ (%)	23.9
R_{free}‡ (%)	30.0
No. of residues	648
No. of water molecules	23
Mean protein B factor (Å^2)	67.0
Mean solvent B factor (Å^2)	42.9
Mean papaverine B factor, monomer A (Å^2)	81.3
Mean papaverine B factor, monomer B (Å^2)	86.2
R.m.s.d. bond lengths (Å)	0.007
R.m.s.d. bond angles (°)	1.05
Ramachandran plot statistics (%)	
Residues in most favoured regions	90.6
Residues in additional allowed regions	9.4

† $R_{merge} = \sum_{hkl}\sum_i |I_i(hkl) - \langle I(hkl)\rangle| / \sum_{hkl}\sum_i I_i(hkl)$, where $I_i(hkl)$ is the intensity measurement for reflection i and $\langle I(hkl)\rangle$ is the mean intensity for multiply recorded reflections. ‡ R_{work}, $R_{free} = \sum_{hkl} ||F_{obs}| - |F_{calc}|| / \sum_{hkl} |F_{obs}|$, where the working and free R factors are calculated using working and free reflections, respectively.

3. Results and discussion

3.1. The structure of hPDE10a in complex with papaverine

The hPDE10a–papaverine complex has two protein monomers in the asymmetric unit, with one papaverine molecule bound in the active site of each monomer. Unexpectedly, the papaverine binding in monomer *A* is very different when compared with the binding in monomer *B* (Figs. 1 and 2*a*, respectively). Papaverine binding in monomer *B* (Fig. 1) is likely to represent the true mode of binding, superimposing well with the binding of a tetrahydroisoquinolinyl dimethoxyquinazoline derivative (Fig. 2*b*) in a rat PDE10a crystal structure (PDB code 2o8h; Chappie *et al.*, 2007). In monomer *B*, a bidentate hydrogen-bonding interaction is formed between the methoxy groups of the isoquinoline which share the hydrogen donor Gln726, similar to the interaction observed in PDB entry 2o8h. Moreover, stacking interactions are formed between the isoquinoline group and phenylalanines 696 and 729, with the papaverine phenyl group packing against the side of Phe729 (Fig. 1). The papaverine binding to monomer *A* is likely to present an artefact resulting from the cross-linking (discussed in §3.2).

3.2. Effects of cross-linking on hPDE10a crystals and papaverine binding

Native hPDE10a crystals immediately cracked upon soaking with papaverine, whilst hPDE10a crystals cross-linked using glutaraldehyde were able to withstand soaking for several hours. The increased internal strength of cross-linked hPDE10a crystals was further verified as the crystals were able to withstand soaking in pure water for several hours. The hPDE10a–papaverine protein backbone

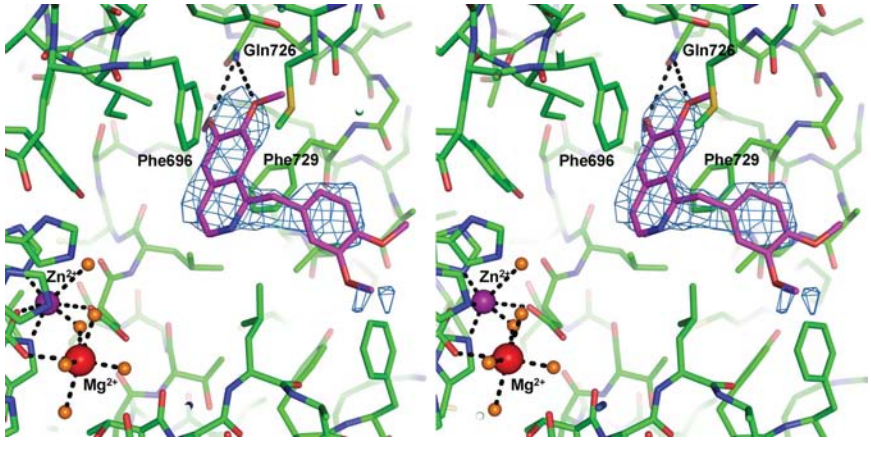

Figure 1
Stereo figure of the active site of monomer *B* in the hPDE10a–papaverine crystal structure. $F_o - F_c$ electron density is contoured at 2.0σ. Hydrogen-bonding interactions are shown as dotted lines to Gln726. The protein and papaverine are shown as a stick models with green and magenta C atoms, respectively. Zinc and magnesium are shown as purple and red spheres, respectively.

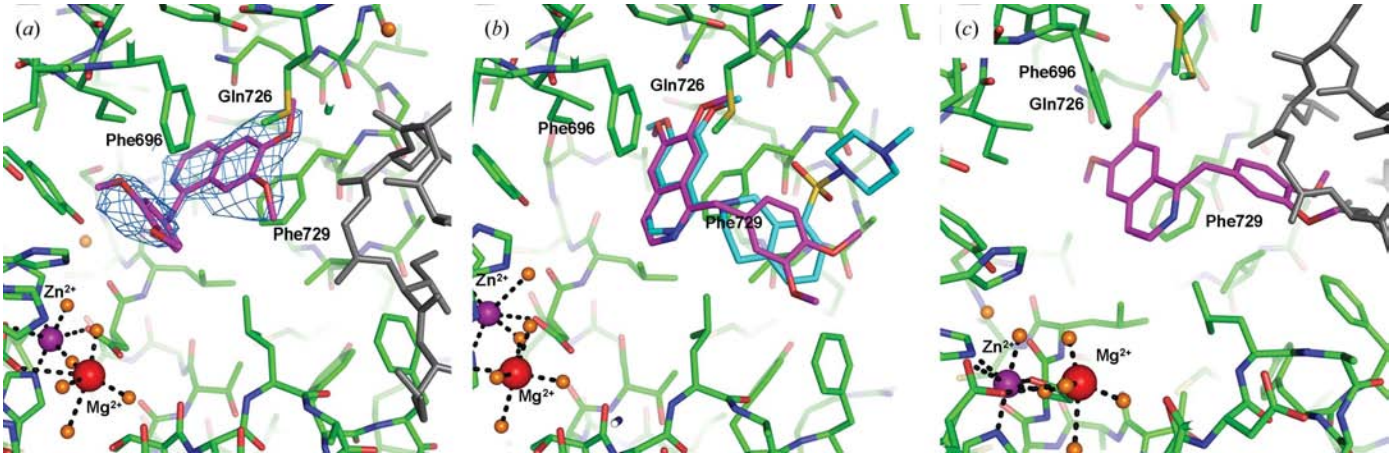

Figure 2
Papaverine modes of binding in the active site of hPDE10a. (*a*) Papaverine binding to monomer *A*. $F_o - F_c$ electron density is contoured at 2.0σ. (*b*) Superposition of a tetrahydroisoquinolinyl dimethoxyquinazoline derivative (shown with cyan C atoms) in a rat PDE10A crystal structure (PDB entry 2o8h) onto monomer *B* of the hPDE10a complex. (*c*) Superposition of papaverine bound to monomer *B* onto monomer *A* reveals a steric hindrance with a neighbour molecule to monomer *A* (shown as a grey stick model). The protein and papaverine are shown as stick models with green and magenta C atoms, respectively. Zinc and magnesium are shown as purple and red spheres, respectively.

in the refined structure superimposes well with the backbone of the published hPDE10a structure (C^{α} r.m.s. displacement of 0.4 and 1.2 Å, respectively, for monomers *A* and *B*) and hence the cross-linking does not lead to detectable differences in the overall structure. However, cross-linked hPDE10a crystals diffracted to a lower resolution (∼2.8 Å) when compared with native crystals (∼2.3 Å). Inspection of the electron-density maps showed no evidence of glutaraldehyde bound to any of the lysine residues.

Comparison of papaverine binding to monomers *A* and *B* with the crystal structure of rat PDE10a complexed with a tetrahydroisoquinolinyl dimethoxyquinazoline derivative (Chappie *et al.*, 2007) shows that papaverine binding to monomer *B* represents a plausible mode of binding, retaining the hydrogen-bonding pattern with Gln726. Furthermore, its dimethoxyisoquinoline and dimethoxyphenyl groups overlap with the dimethoxyquinazoline and tetrahydroisoquinoline groups, respectively (Fig. 2*b*). A similar diether-glutamine hydrogen-bonding pattern is conserved in numerous PDE–ligand complexes in the Protein Data Bank. Conversely, the papaverine in monomer *A* does not generate any hydrogen-bonding interactions with the protein (Fig. 2*a*) and its orientation does not resemble the mode of binding of the 4-amino-6,7-dimethoxyquinazoline series or any other ligand in reported phosphodiesterase structures. The active site of monomer *B* is not in the vicinity of any crystallographic neighbour molecule. However, superimposing papaverine bound to monomer *B* onto monomer *A* (Fig. 2*c*) reveals a steric hindrance with a crystallographic neighbour molecule to monomer *A*, suggesting that the true mode of binding of papaverine observed in monomer *B* cannot be accommodated within monomer *A*. Hence, it is likely that the papaverine mode of binding to monomer *A* is an artefact of crystal contacts in the cross-linked crystal. The steric hindrance explains why cocrystallization of the complex using the crystallization conditions for the apoenzyme alone was not successful. Furthermore, it explains the observation that non-cross-linked crystals dissolve upon soaking of papaverine as a result of the disruption of these crystal contacts upon papaverine binding with its true mode of binding to monomer *A*. Moreover, soaking of numerous ligand fragments that bind between Phe729 and Phe696 and hence do not interfere with the crystal packing was successful using crystals that were not cross-linked (data not shown).

This study exemplifies the cross-linking of protein crystals as an aid to determining ligand complexes in cases with unfavourable crystal-packing interactions for soaking experiments but also highlights the requirement for caution when analysing ligand modes of binding from cross-linked crystals. The method is likely to be applicable to similar crystallographic systems where routine cocrystallization and soaking trials have been unsuccessful.

References

Chappie, T. A., Humphrey, J. M., Allen, M. P., Estep, K. G., Fox, C. B., Lebel, L. A., Liras, S., Marr, E. S., Menniti, F. S., Pandit, J., Schmidt, C. J., Tu, M., Williams, R. D. & Yang, F. V. (2007). *J. Med. Chem.* **50**, 182–185.
Emsley, P. & Cowtan, K. (2004). *Acta Cryst.* D**60**, 2126–2132.
Evans, P. (2006). *Acta Cryst.* D**62**, 72–82.
Leslie, A. G. W. (2006). *Acta Cryst.* D**62**, 48–57.
Lugnier, C. (2006). *Pharmacol. Ther.* **109**, 366–398.
Lusty, C. J. (1999). *J. Appl. Cryst.* **32**, 106–112.
Murshudov, G. N., Vagin, A. A. & Dodson, E. J. (1997). *Acta Cryst.* D**53**, 240–255.
Siuciak, J. A., Chapin, D. S., Harms, J. F., Lebel, L. A., McCarthy, S. A., Chambers, L., Shrikhande, A., Wong, S., Menniti, F. S. & Schmidt, C. J. (2006). *Neuropharmacology*, **51**, 386–396.
Vagin, A. & Teplyakov, A. (1997). *J. Appl. Cryst.* **30**, 1022–1025.
Wang, H., Liu, Y., Hou, J., Zheng, M., Robinson, H. & Ke, H. (2007). *Proc. Natl Acad. Sci. USA*, **104**, 5782–5787.
Wine, Y., Cohen-Hadar, N., Freeman, A. & Frolow, F. (2007). *Biotechnol. Bioeng.* **98**, 711–718.